Benavente Martínez, R.; Salvador Moya, MD. (2013). Influence of the feedstock characteristics on the microstructure and properties of Al2O3 TiO2 plasma-sprayed coatings. Surface and Coatings Technology. 220:74-79. doi:10.1016/j.surfcoat.2012.09.042.

INFLUENCE OF THE FEEDSTOCK CHARACTERISTICS ON THE MICROSTRUCTURE AND PROPERTIES OF Al_2O_3-TiO_2 PLASMA-SPRAYED COATINGS

M. Vicent[1], E. Bannier[1], R. Benavente[2], M.D. Salvador[2], T. Molina[3],R. Moreno[3], E. Sánchez[1]

(1) Instituto de Tecnología Cerámica - Asociación de Investigación de las Industrias Cerámicas. Universitat Jaume I. Av. Vicent Sos Baynat s/n, 12006 Castellón, Spain.
(2) Universidad Politécnica de Valencia. Instituto de Tecnología de Materiales. Camino de Vera s/n, 46022 Valencia, Spain.
(3) Instituto de Cerámica y Vidrio (ICV). CSIC. c/ Kelsen 5, 28049 Madrid, Spain.

Abstract

Atmospheric plasma spraying (APS) is an interesting technique to obtain nanostructured coatings due to its versatility, simplicity and relatively low cost. However, nanometric powders can not be fed into the plume using conventional feeding systems, due to their low mass and poor flowability, and must be adequately reconstituted into sprayable micrometric agglomerates.

In this work, Al_2O_3-13wt%TiO_2 nanostructured and submicron powders were deposited using APS. The feedstocks were obtained by spray drying from two starting suspensions, prepared by mixing two commercial nanosuspensions of Al_2O_3 and TiO_2, or by adding nanometric TiO_2 and submicron Al_2O_3 powders to water. The spray-dried granules were heat-treated to reduce their porosity and the resultant powders were fully characterised.

Optimisation of the deposition conditions enabled the reconstituted powders to be successfully deposited, yielding coatings that were well bonded to the substrate. The coating microstructure, characterised by SEM, was formed by semi-molten feedstock agglomerates surrounded by fully molten particles that act as a binder.

Moreover, microhardness, adhesion, and tribological behaviour were determined, and the impact of the granule properties on these properties was studied. It was found that changing the feedstock characteristics allows to control the coating quality and properties.

1 Introduction

Plasma spraying, a type of thermal spray technique, is broadly used in industry for obtaining coatings. Nanostructured ones exhibit better performance than their conventional counterparts [1-5]. Unluckily, nanoparticles cannot be fed directly into the plasma torch and need to be agglomerated into a sprayable powder [6-8]. Commonly, agglomeration of nanoparticles takes place by spray drying [6-11] or freeze-drying [11] of a nanoparticle suspension, frequently followed by thermal treatment of the granules in order to decrease their porosity [6,8]. Previously to the agglomeration step, the most difficult task is to disperse nanoparticles in water and prepare stable nanosuspensions [9-10].

Plasma sprayed alumina-based ceramic coatings are used in a variety of applications to provide electrical insulation, increased wear resistance, and chemically unreactive surfaces [12]. Al_2O_3-TiO_2 coatings fabricated with nanopowders show very promising bonding strength and wear resistance when compared with conventional feedstock as reported elsewhere [13]. Moreover, the Al_2O_3-TiO_2 nanostructured coatings containing 13 wt% TiO_2 showed the most excellent wear resistance among the Al_2O_3-TiO_2 ones [14]. Although, many research effort has been made to pass from the micro-scale to the nano-scale using both powders or liquids as feedstock [1], very few studies deals with submicron-sized feedstock [15].

In this work, Al_2O_3 - 13 wt% TiO_2 coatings were obtained by atmospheric plasma spraying (APS) using commercial powders (micrometric and nanostructured) and reconstituted granules (obtained by spray-drying, from stable suspensions).

In previous research, it was found that the nanostructured spray-dried agglomerates obtained from concentrated suspensions yielded coatings with lower void content than those obtained using powders from less concentrated suspensions [8]. However, feedstocks made up of powders with bimodal particle size distribution (submicron-nano particles) were not explored.

This work deals with the relationship between reconstituted granules characteristics and the properties of nanostructured coatings prepared by APS using different feedstocks. Complete characterization of feeding powders (FEG-ESEM, granule size distribution, flowability and

apparent density) and newly developed nanostructured coatings (microstructure by SEM and mechanical properties such as microhardness, toughness, wear and pull-off) was performed.

2 Materials and methods

2.1 Feedstock preparation

Two nanopowder suspensions of alumina and titania (VP Disp. W630X and AERODISP® W740X respectively, Degussa-Evonik, Germany), a submicron-sized powder of alumina (Condea-Ceralox HPA-0.5, Sasol, USA) and a nanopowder of titania (AEROXIDE® P25, Degussa-Evonik, Germany) were used as raw materials.

First, a 10 vol.% of Al_2O_3–13 wt% TiO_2 nanosuspension was prepared by mixing both commercial suspensions [8]. Secondly, a 30 vol.% of Al_2O_3–13 wt% TiO_2 submicron-nano suspension was prepared by dispersing nanosized titania particles and submicronic alumina particles in water. A commercial polyacrylic acid-based polyelectrolyte (DURAMAX™ D-3005, Rohm & Haas, USA) was used as deflocculant [10,16].

In both cases, stable, well-dispersed and low-viscosity suspensions were obtained. Both suspensions were then reconstituted into sprayable granules in 2 steps:

a) Spray-drying. Spray-dried agglomerates were obtained in a spray dryer (Mobile Minor, Gea Niro, Denmark) [8,10,11].

b) Thermal treatments. In order to obtain denser granules, the spray-dried powders were heat treated in an electric kiln with soaking time of 60 minutes, at 1250 ºC for the powder obtained from nanoparticles suspension (feedstock N10) [8], and at 1200 ºC for the powder obtained from the submicron-nano particles suspension (feedstock SN30).

Finally, and for comparison purposes, two commercial feedstocks with the same Al_2O_3–TiO_2 weight ratio, were also deposited: a conventional microstructured one (Metco 130, Sulzer Metco, Germany), referred as CM, and a nanostructured one (Nanox™ S2613S, Inframat Advanced Materials, USA), referred as CN.

2.2 Feedstock characterization techniques

A field-emission gun environmental scanning electron microscope, FEG-ESEM (QUANTA 200FEG, FEI Company, USA) was used to examine the feedstock microstructure. Moreover, granule size distribution was measured by laser light scattering (Mastersizer S, Malvern, UK). Finally, powder flowability was evaluated in terms of the Hausner ratio, defined as the ratio of the tapped density to the apparent (or poured) density of the powder, and agglomerate apparent density was calculated from tapped powder density by assuming a theoretical packing factor of 0.6, which is characteristic of monosize, spherical particles [17].

2.3 Coating deposition

Al_2O_3–13 wt% TiO_2 coatings were deposited by APS on metallic substrates (AISI 304) prepared as set out elsewhere [4]. The plasma spray system consisted of a gun (F4-MB, Sulzer Metco, Germany) operated by a robot (IRB 1400, ABB, Switzerland). The deposition was made using argon and hydrogen as plasma-forming gases. The same spraying conditions were used in all deposition experiments: Ar flow=35 slpm, H_2 flow=12 slpm, arc intensity=600 A, spraying distance=0.12 m, spraying velocity=1 m/s.

2.4 Coating characterization techniques

First, the coating microstructures were observed by SEM (JSM6300, JEOL, Japan). Coating porosity was evaluated by image analysis from ten backscattered electron mode micrographs.

The hardness and fracture toughness of the materials were determined using an indentation technique. A conventional diamond pyramid indenter (Vickers) was fit to the piece of equipment (4124, INNOVATEST, Netherlands) and a load of 3 N was applied for 15 s according to the standard specification ASTM E92-72.

Wear tests were carried out under dry sliding conditions using a pin-on-disk tribometer (MT2/60/SCM/T, Microtest, Spain) in accordance with ASTM wear testing standard G99-03. As friction partner, 5 mm diameter-Si_3N_4 ball was used. The normal load, sliding speed and distance were fixed at 10 N, 0.1 m/s and 1000 m, respectively. Testing was carried out in air, at room temperature and in dry conditions. Prior to measuring hardness, toughness and wear, the

samples were polished (RotoPol-31, Struers, Denmark) with diamond to 1 μm roughness for hardness and toughness, and with SiC to 2-3 μm for wear.

The pull-off tests were performed according to ASTM D4541 in a PosiTest (AT-A, DeFelsko, USA). The dolly, whose diameter was 10 mm, was attached to the coating surface with a curable epoxy adhesive for 8 h. After that, the dolly was vertically pulled-off (with a rate 2.0 MPa) while measuring the necessary force. The results are the averages of 3 repeated tests done on each sample.

3 Results and discussion

3.1 Feedstock characterization

A former study revealed that the conventional powder (CM) is formed by angular particles between 20 and 60 μm, while the nanostructured feedstock (CN) contained highly porous agglomerates of nanoparticles [4]. Moreover, both reconstituted feedstock are made of spherical spray-dried granules composed by nanoparticles for N10, and by ordered nano and submicron-sized particles for SN30 (Figure 1). The mixing of two particles sizes in SN30 leads to a compacting effect and, therefore, to a much higher agglomerate apparent density (Table 1).

Figure 2 shows the granule size distribution of all feedstocks, which exhibit similar monomodal granule size distribution. This demonstrates that the prepared suspensions are homogeneous, even in the case of SN30 sample, where nano- and submicron-sized particles are randomly distributed.

Table 1 details the principal characteristics of all the feedstocks (commercial and reconstituted), including average granule size (measured by laser diffraction), Hausner ratio and agglomerate apparent density.

On one hand, granule apparent densities were 3800 and 2000 kg/m^3 for CM and CN, respectively. Indeed, CM is a fused and crushed dense powder, whereas CN is spray-dried porous powder. On the other hand, agglomerate apparent densities of the reconstituted feedstock were 1700 kg/m^3 for N10 and 3100 kg/m^3 for SN30, as a consequence of the better packing

efficiency inside the agglomerate associated with the submicrometric-nanometric particle arrangement.

Moreover, the Hausner ratio for all powders was ≤ 1.25, indicating good flowability and confirming that both reconstituted feedstocks are appropriate for APS process [8,10].

Finally, commercial powders (CM and CN) contained smaller granules than reconstituted ones (N10 and SN30).

3.2 Coating microstructure

The coatings microstructure is clearly influenced by the feedstock characteristics, as revealed by SEM observations (Figures 3 and 4). As expected, the coating obtained from the conventional powder (CM) shows a typical splat-like microstructure, formed by successive impacts of fully molten droplets. However, the layers deposited from both nanostructured powders (CN and N10) exhibit a bimodal microstructure formed by partially molten agglomerates, that retained the initial nanostructure, surrounded by a fully molten matrix. Such microstructure has been reported in literature [4]. Moreover, sample SN30 also displayed a few partially molten areas, which are made of bigger particles than in the former case, as the feedstock mainly contained submicron particles. Yet, it has to be pointed out that these coatings are mainly formed by fully molten areas, as a consequence of the high sintering grade of the initial granules.

Differences were also found in the coating porosity as reported in table 2. The coatings obtained from both commercial powders presented a lower porosity probably due to their smaller average granule size. Indeed, smaller granules are easier to melt, giving raise to more deformable droplets, and consequently to lower coating porosity.

3.3 Coating mechanical properties

Coatings mechanical properties are given in table 2.

The conventional layer displays the highest adhesion strength, while the other 3 coatings exhibit similar values. Such results can be explained by the morphology of the conventional feedstock, which is a dense “fused and crushed” powder instead of a porous spray-dried material. Actually it should display a higher thermal conductivity, leading to an increased melting grade during

deposition and though, to a superior deformability of the droplets when they impact against the substrate, resulting in improved adhesion strength.

Moreover, nanostructured coatings (CN and N10) displayed somehow lower fracture toughness than that of conventional and submicron-nanometric ones. Such results is in contradiction with the common hypothesis which suggests that the presence of partially molten nanozones can impede the propagation of cracks in nanostructured plasma-sprayed layers, since the fracture toughness of agglomerates should be higher than that of the matrix [18]. Actually, as confirmed by the SEM observations (Figure 4), the partially molten areas found in this study are highly porous, and exhibit low cohesion between the nanoparticles. As a consequence, cracks may propagate easily between the nanoparticles explaining the lower fracture toughness. This poor cohesion of the nanozones is probably due to the low density of the granules found in the corresponding feedstocks (Table 1).

Furthermore, significant differences were observed in the microhardness of the coatings, which varied from 2.2 GPa, for the conventional layer, up to 9.5 GPa, for SN30 coating. Besides, it can be observed that, when the microhardness increases, the wear resistance of the coating is improved. In fact, the best wear performance was found for SN30 coating while CM layer displayed the highest wear loss. Both nanostructured coatings (CN and N10) show an intermediate behaviour, with a significantly higher wear resistance than that of the conventional layer.

In spite of the existence of some correlation between microhardness and wear resistance (Figure 5), it has to be pointed out that the fracture toughness also plays a key role, as both deformation and microfracture are usually involved in wear mechanisms. Actually, the ratio between hardness (resistance to deformation) and fracture toughness (resistance to fracture), called brittleness index (B) [19], can be used to determine the relative wear resistance of bulk materials [20]. In this study, it was found that the wear loss of the coatings decreases when their brittleness index increases, with a linear relationship between both magnitudes (Figure 5). Such results are in accordance with the study made by Boccaccini [20], which established that for low values of the brittleness index ($B < 4\ \mu m^{-1/2}$) the wear rate is reduced when B is increased, as in

such conditions the mechanisms of material removal involve both plastic deformation and microfracture. As a consequence, it may be interesting to take into account the brittleness index, instead of hardness or fracture toughness separately, to explain the wear behaviour of thermal-sprayed coatings.

4 Conclusions

In this study, four different Al_2O_3–13 wt% TiO_2 feedstocks have been deposited by APS: a fused and crushed conventional powder, a commercial nanostructured spray-dried powder and two reconstituted powders. Both reconstituted feedstocks were prepared by spray-drying and subsequent thermal treatment from stabilized aqueous suspension obtained, in one case, by mixing two commercial nanoparticles suspensions, and in the other case, by dispersing TiO_2 nanoparticles and Al_2O_3 submicron-sized particles into water.

In general, the coatings obtained from the submicron-nanometric reconstituted powder leads to better coatings properties whereas the conventional coatings display the worst wear behaviour.

Finally, it should be highlighted that coating microstructure and properties are clearly influenced by the feedstocks characteristics, which demonstrates that the initial powder properties should be optimized, along with the spraying parameters, in order to obtain coatings with superior performances.

ACKNOWLEDGEMENTS

This work has been supported by the Spanish Ministry of Science and Innovation (project MAT2009-14144-C03).

REFERENCES

[1] FAUCHAIS P.; VARDELLE M.; COUDERT J.F.; VARDELLE A.; C. DELBOS; FAZILLEAU J. *Pure Appl. Chem.*, 77(2), 475–485, 2005.

[2] LIMA R.S.; MARPLE B.R. *J. Therm. Spray Technol.*, 16(1), 40-63, 2007.

[3] PAWLOWSKI L. *Surf. Coat. Technol.*, 202(18), 4318-4328, 2008.

[4] SÁNCHEZ E.; CANTAVELLA V.; BANNIER E.; SALVADOR M.D., KLYASTKINA E., MORGIEL J.; GRZONKA J.; BOCCACCINI A. *J. Therm. Spray Technol.*, 17(3), 329-337, 2008.
[5] RICO A.; POZA P.; RODRÍGUEZ J. *Vacuum* [DOI: 10.1016/j.vacuum.2012.01.008].
[6] SHAW L.L.; U, GOBERMAN D.; REN R.; GELL M.; JIANG S.; WANG Y.; XIAO T.D.; STRUTT P.R. *Surf. Coat. Technol.*, 130(1), 1-8, 2000.
[7] GELL M.; JORDAN E.H.; SOHN Y.H.; GOBERMAN D.; SHAW L.; XIAO T.D. *Surf. Coat. Technol.*, 146–147, 48-54, 2001.
[8] SÁNCHEZ E.; MORENO A.; VICENT M.; SALVADOR M.D.; BONACHE V.; KLYATSKINA E.; SANTACRUZ I.; MORENO R. *Surf. Coat. Technol.*, 205(4), 987–992, 2010.
[9] FAZIO S.; GUZMÁN J.; COLOMER M.T.; SALOMONI A.; MORENO R. *J. Eur. Ceram. Soc.*, 28(11), 2171-2176, 2008.
[10] VICENT, M.; SÁNCHEZ, E.; MORENO, A.; MORENO, R. Preparation of high solids content nano-titania suspensions to obtain spray-dried nanostructured powders for atmospheric plasma spraying. *J. Eur. Ceram. Soc.*, 32(1), 185-194, 2012.
[11] VICENT, M.; SÁNCHEZ, E.; MOLINA T.; NIETO M.I.; MORENO R. *J. Eur. Ceram. Soc.*, 32(5), 1019-1028, 2012.
[12] GUILEMANY, J.M.; NUTTING, J.; DOUGAN, M.J. *J. Therm. Spray Technol.*, 6(4), 425-429, 1997.
[13] AHN J.; HWANG B.; SONG E.P.; LEE S.; KIM N.J. *Metall. Mater. Trans. A*, 37A, 1851-1861, 2006.
[14] LIN X.; ZENG Y.; LEE S.W.; DING, C. *J. Eur. Ceram. Soc.*, 24(4), 627-634, 2004.
[15] DARUT, G.; AGEORGES, H.; DENOIRJEAN, A.; MONTAVON, G. ; FAUCHAIS, P. *J. Therm. Spray Technol.*, 17(5-6), 788-795, 2008.
[16] MOLINA T.; VICENT M.; SÁNCHEZ E.; MORENO R. *Mater. Res. Bull.* [accepted].
[17] AMORÓS J.L.; BLASCO A.; ENRIQUE J.E.; NEGRE F. *Bol. Soc. Esp. Ceram. Vidr.*, 26(1), 31-37, 1987.
[18] BANSAL, P.; PADTURE, N.P.; VASILIEV, A., *Acta Mater.*, 51(10-11), 2959-2970, 2003.
[19] LAWN, B.R.; MARSHALL, D.B. *J. Am. Ceram. Soc.*, 62(7-8), 347-350, 1979.
[20] BOCCACCINI, A.R. *Interceram*, 48(3), 176-187, 1999.

TABLES

Table I. Main characteristics of the powders (commercial ones and spray-dried granules obtained from nanosuspensions and from submicron-nano suspensions)

Reference	Laser diffraction	Powder flowability	
	$D_{v,\,0.5}$ (µm)	Hausner ratio	Agglomerate apparent density (kg/m^3)
CM	36	1.28	3800
CN	38	1.19	2000
N10	70	1.20	1700
SN30	57	1.25	3100

Table II. Coatings properties

	CM	CN	N10	SN30
Porosity (%)	3	3	8	6
Adhesion strength (MPa)	10.0	7.5	7.8	7.7
Vickers microhardness (GPa)	2.2	4.2	5.3	9.5
Fracture Toughness ($MPa \cdot m^{1/2}$)	1.10	0.59	0.60	1.00
Wear loss ($10^{-10} \cdot kg/mN$)	1.76	0.39	0.29	0.08
Brittleness Index ($\mu m^{-1/2}$)	0.0020	0.0071	0.0088	0.0095

FIGURE CAPTIONS

Figure 1. FEG-ESEM micrographs, at two magnifications, of spray-dried granules after calcination

Figure 2. Granule size distribution measured by laser light scattering

Figure 3. SEM micrographs showing the general microstructure of all as-sprayed coatings, partially molten areas are referred as “pm”

Figure 4. High magnification SEM micrographs of the partially molten areas found in coatings CN, N10 and SN30

Figure 5. Evolution of the wear loss as a function of the microhardness or of the brittleness index

FIGURES

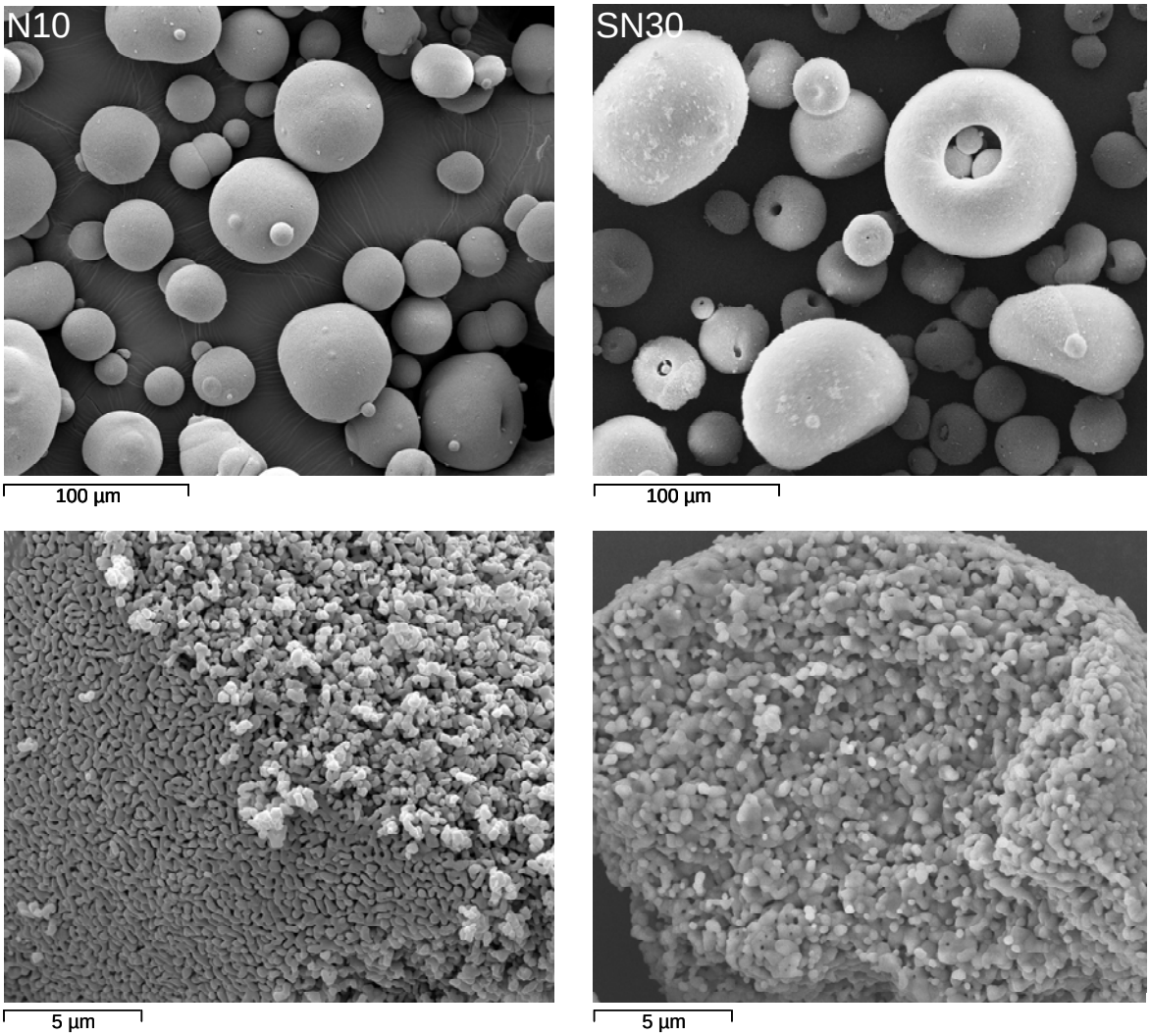

Figure 1

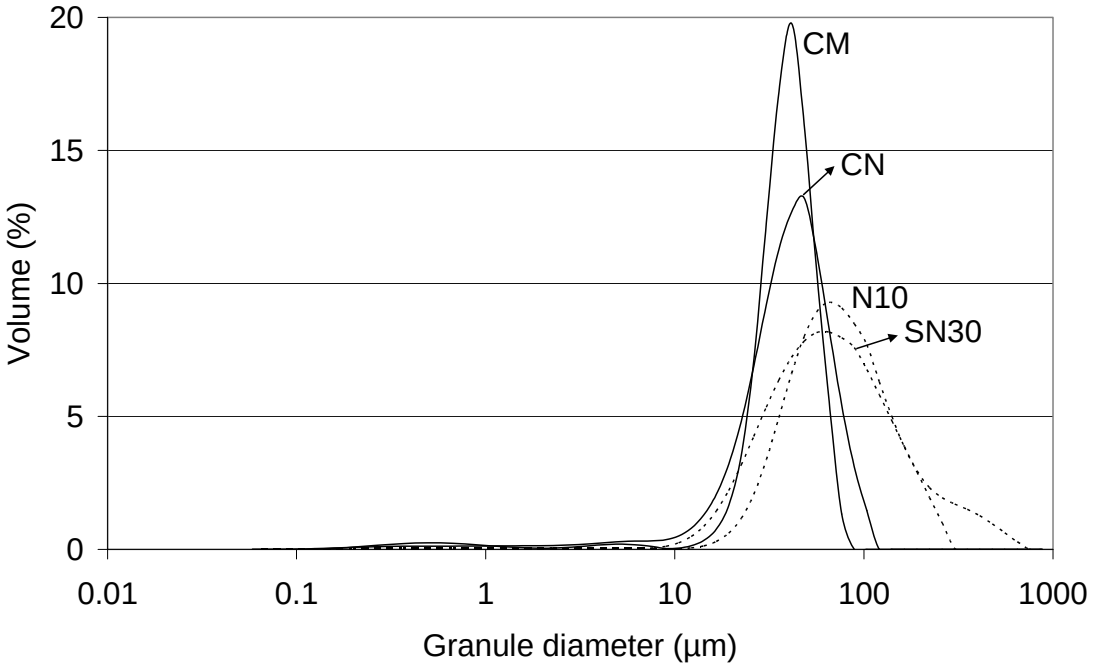
20
15
10
5
0
Volume (%)
CM
CN
N10
SN30
0.01
0.1
1
10
100
1000
Granule diameter (µm)

Figure 2

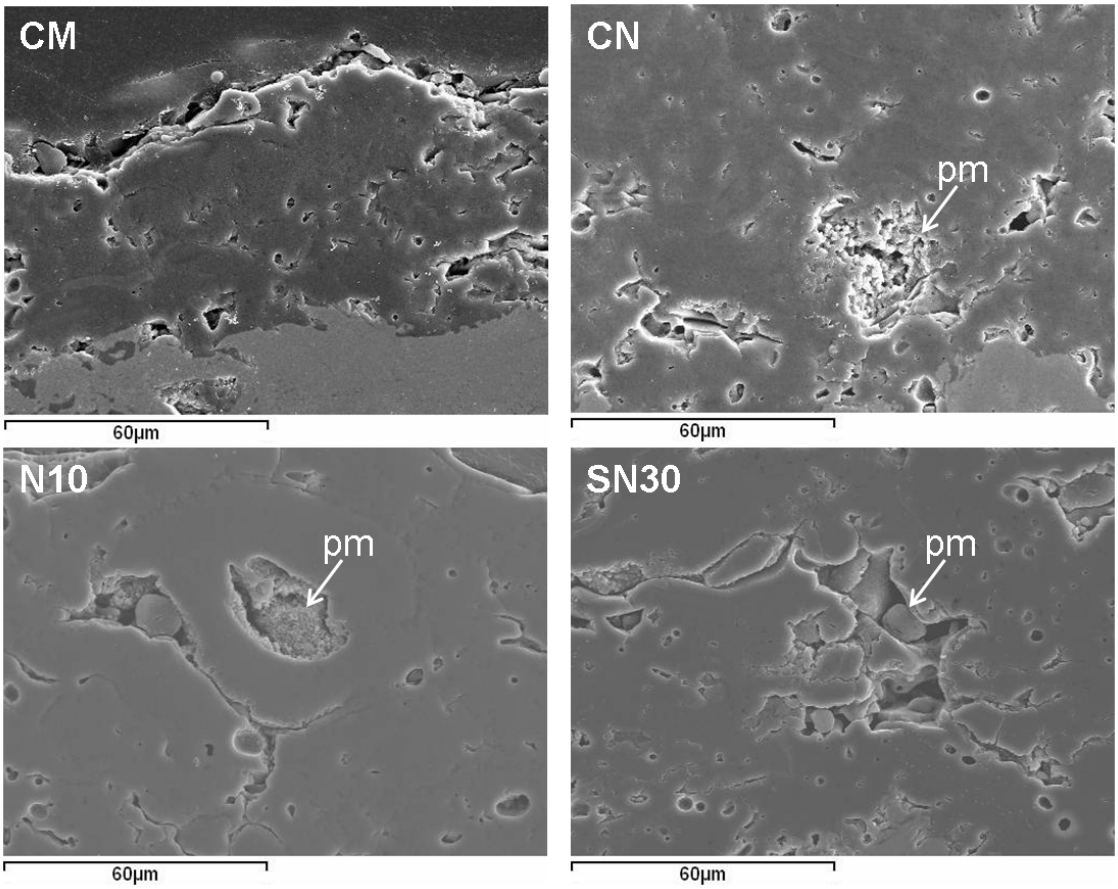

Figure 3

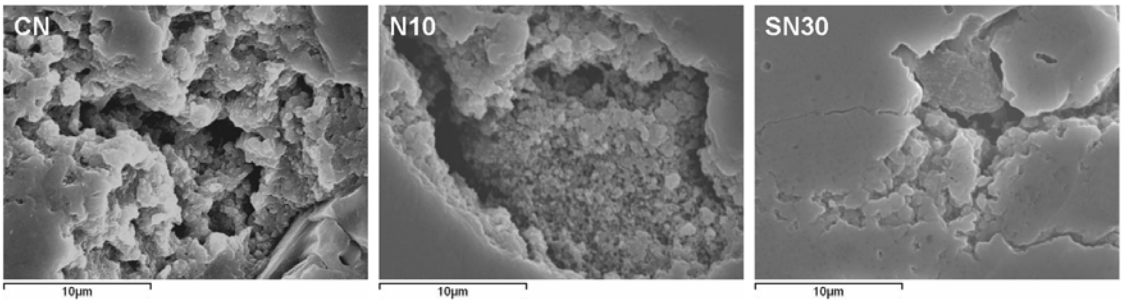

Figure 4

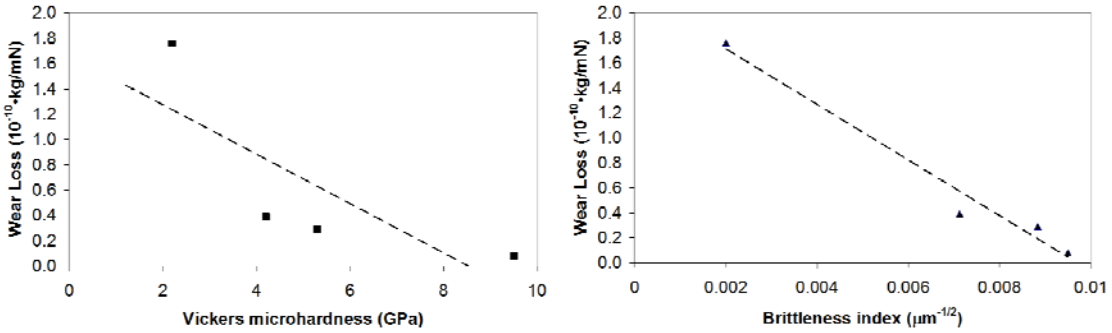
Wear Loss (10^{-10}•kg/mN)
2.0
1.8
1.6
1.4
1.2
1.0
0.8
0.6
0.4
0.2
0.0
0
2
4
6
8
10
Vickers microhardness (GPa)
Wear Loss (10^{-10}•kg/mN)
2.0
1.8
1.6
1.4
1.2
1.0
0.8
0.6
0.4
0.2
0.0
0
0.002
0.004
0.006
0.008
0.01
Brittleness index ($\mu m^{-1/2}$)

Figure 5